

1
2
3
4
5
6
7
8
9
10
11
12
13
14
15
16
17
18
19

**Estimating the van Genuchten retention curve parameters of undisturbed soil
from a single upward infiltration measurement**

D. Moret-Fernández ^a, C. Peña-Sancho ^a, B. Latorre ^a, Y. Pueyo ^b, M.V. López ^a

^a *Departamento de Suelo y Agua, Estación Experimental de Aula Dei, Consejo Superior de
Investigaciones Científicas (CSIC), PO Box 13034, 50080 Zaragoza, Spain*

^b *Instituto Pirenaico de Ecología (CSIC), Av. Montañana 1005, P.O. Box 13.034, 50080 Zaragoza,
Spain*

* Corresponding author. Tel.: (+34) 976 716140; Fax: (+34) 976 716145

E-mail address: david@eead.csic.es

Abstract

Estimation of the soil-water retention curve, $\theta(h)$, on undisturbed soil samples is of paramount importance to characterise the hydraulic behaviour of soils. Moret-Fernández and Latorre (2016) presented a method to determine the parameters of the van Genuchten (1980) water retention curve (α and n) from the saturated hydraulic conductivity (K_s), the sorptivity (S) and the β parameter of the Haverkamp et al. (1994) model, calculated S and β from the inverse analysis of an upward infiltration. Although this inexpensive, fast and simple to implement method was satisfactorily applied to sieved soil samples, its applicability on undisturbed soils has not been tested. The objective of this work is to show that the method can be applied to undisturbed soil cores representing a range of textures and structures. The undisturbed soil cores were collected with 5 cm-internal diameter -i.d.- by 5 cm-high stainless steel cylinders sampled on structured soils located in two different places: agricultural loam soil under conventional, reduced and no tillage systems, and a loam soil under grazed and ungrazed natural shrubland. The α and n values estimated for the different soils with the upward infiltration method (UI) were compared to corresponding values calculated with TDR-pressure cells (PC), for pressure heads of -0.5, -1.5, -3, -5, -10, -50 kPa. To compare both methods, the α values measured with UI were calculated to the drying branch of $\theta(h)$. Three replications of upward infiltration and PC were performed per treatment. The results demonstrated that the 5 cm-high cylinders used in all experiments provided accurate estimates of S and β . Overall, the α and n values estimated with UI were larger than those measured with PC. These differences could be attributed in part to limitations of the PC method. On average, the n values calculated from the optimized S and β data were 5% larger than those obtained with the TDR-pressure cell. A relationship with a slope close to one fitted the n values estimated with both methods ($n_{PC} = 0.73 n_{UI} + 0.49$; $R^2 = 0.78$; $p < 0.05$). The results showed that this method can be a promising technique to estimate the hydraulic properties on undisturbed soil samples

44

45 **Keywords:** Hydraulic conductivity; Sorptivity, Soil tillage.

46

47 **1.- INTRODUCTION**

48 Water flow in the vadose zone is mainly regulated by the unsaturated hydraulic conductivity, K ,
49 which is related to the water retention curve, $\theta(h)$ (van Genuchten, 1980). Those parameters are
50 indispensable to simulate soil water processes, such as water erosion, soil pollutant movement, or
51 nutrient dynamics. While K reflects the ability of soil to transmit water when the soil is submitted to a
52 hydraulic gradient, the water retention curve defines the relationship between the soil volumetric
53 water content (θ) ($L^3 L^{-3}$) and the matric potential h (L). The unimodal van Genuchten (1980)
54 equation relates θ and h through two empirical variables: n and α .

55 Laboratory methods used to characterize $\theta(h)$ can be classified into two categories, direct
56 experimental and indirect inferential methods. The main direct laboratory methods are the pressure
57 extractor (Klute, 1986), which estimates $\theta(h)$ from pairs of measured h and θ values, or the
58 evaporative method, that calculates the K and $\theta(h)$ from the pressure head response of two
59 tensiometers placed at different depths (Gardner and Miklich, 1962). Although these techniques can
60 be applied on undisturbed soil cores, the tediousness of the experiments together with the specific
61 equipment needed can limit its use. The indirect methods, which are increasingly employed and
62 involve inverse solutions of the Richard's equation, estimate the soil hydraulic properties from the
63 numerical analysis of measured transient soil properties (i.e., water flow, soil pressure head). The
64 main advantage of these techniques is the ability to simultaneously estimate K and $\theta(h)$. To date,
65 many different indirect procedures have been developed. Simunek et al. (1998) employed the
66 evaporation method to estimate the drying branch of the soil hydraulic properties from simultaneous
67 numerical analysis of measured soil water evaporation and soil pressure heads recorded at different

68 depths. Hudson et al. (1996) suggested estimating the wetting branch of the soil hydraulic properties
69 from the inverse analysis of an upward flow experiment under laboratory conditions using a constant
70 flux of water at the bottom of the soil sample. Shao and Horton (1998) developed an integral method
71 that allowed estimating the $\theta(h)$ van Genuchten model parameters from a simple horizontal
72 infiltration experiment on a 20-cm length soil column, followed by measuring the saturated hydraulic
73 conductivity. Young et al. (2002) employed a Mariotte system and tensiometers installed in a 15-cm-
74 long soil column to estimate the wetting branch of the soil hydraulic properties. Moret-Fernández et
75 al. (2016b) developed a tension sorptivimeter that allowed estimating the soil hydraulic parameters
76 from the inverse analysis of a multiple tension upward infiltration curve, without using tensiometers.
77 Taking into account the hysteresis phenomena, Peña-Sancho et al. (2017) estimated the soil hydraulic
78 properties from a capillary wetting process at saturation followed by an evaporation process. Finally,
79 Moret-Fernández and Latorre (2016) developed a simple procedure to calculate the parameters of the
80 $\theta(h)$ van Genuchten model from a single upward infiltration curve followed by an overpressure step
81 by applying the 1D downward Haverkamp et al. (1994) model adapted for an upward infiltration. In
82 this case, a 5 cm-high cylinder filled with sieved soil was used.

83 Undisturbed soils in field conditions have some unique features in contrast with packed laboratory
84 soils, such as the presence of roots or a complex porous system. Measurements of $\theta(h)$ on
85 undisturbed soil samples are generally preferable to those made on disturbed samples. Current
86 methods developed to estimate $\theta(h)$ have serious limitations when applied to undisturbed soil
87 samples. This is the case of the methods based on the tension measurements, where installation of
88 tensiometers in the undisturbed soil column is delicate and complex (Arya, 2002). Although Han et
89 al. (2010) applied the integral method of Shao and Horton (1998) on undisturbed soil samples, the
90 long soil columns (20 cm) used in the experiment and the need to use transparent cores, may limit its
91 application for soils. In the method developed by Moret-Fernández et al. (2016b), the highly negative
92 pressure head used at the beginning of the experiment, restricted the use to soil samples that had good

93 contact between the nylon mesh of the sorptivimeter and the corresponding mesh located at the
 94 bottom of the soil cylinder (e.g. sieved soils). These authors suggested that this problem could be
 95 solved by starting the experiment at saturation conditions. This limitation could be solved by the
 96 Moret-Fernández and Latorre (2016) method, in which the bottom boundary of the upward
 97 infiltration experiments starts at saturation conditions.

98 It is evident from the above literature that the current methods to estimate the water retention curve
 99 parameters presents several limitations when applied to undisturbed soil samples. Further efforts are
 100 needed to develop alternative methods to estimate the soil hydraulic properties on undisturbed soil
 101 samples. The objective of this paper is to test the applicability of the Moret-Fernández and Latorre
 102 (2016) method to estimate the soil hydraulic properties on undisturbed soil samples. Undisturbed
 103 cores (5 cm i.d. by 5cm-high) were collected in two different fields with different tillage
 104 (conventional, reduced and not tillage) and grazing (natural and grazed) managements, and the
 105 estimated hydraulic parameters were compared to those calculated with TDR- pressure cell (PC).

106

107 **2. MATERIALS AND METHODS**

108 **2.1. Theory**

109 For 1-D upward water flow, the cumulative infiltration, $I_{1D}(t)$ on a homogeneous, uniform initial
 110 water content and infinite length soil column, can be described by the quasi-exact equation derived
 111 from the Haverkamp et al. (1994) formulation (Moret-Fernández and Latorre, 2016)

$$112 \quad \frac{2(1-\beta)\Delta K^2}{S_0^2} t = \frac{2\Delta K(I_{1D} + K_n t)}{S_0^2} - \ln \left\{ \frac{1}{\beta} \exp \left[\frac{2\beta\Delta K(I_{1D} + K_n t)}{S_0^2} \right] + 1 - \frac{1}{\beta} \right\} \quad (1)$$

113 where t is time (T), θ ($L^3 L^{-3}$) is the volumetric water content, S_0 is the sorptivity ($L T^{-0.5}$) for θ_0 ; K_0
 114 and K_n are the hydraulic conductivity values ($L T^{-1}$) corresponding to θ_0 and θ_n , respectively, $\Delta K = K_n -$
 115 K_0 , and β is an integral shape parameter. This model is only suitable for those soils where the

116 saturated-independent shape parameter β ranges between 0.3 and 1.7 (sand, loam and silt)
 117 (Lassabatere et al., 2009). The β shape function is defined as (Haverkamp et al., 1994)

$$\beta = 2 - 2 \frac{\int_{\theta_n}^{\theta_0} (K - K_n / K_0 - K_n)(\theta_0 - \theta_n / \theta - \theta_n) D(\theta) d\theta}{\int_{\theta_n}^{\theta_0} D(\theta) d\theta} \quad (2)$$

118
 119 For saturated soils, the steady state water flux density, q , into the soil ($L T^{-1}$) (Lichtner et al., 1996)
 120 can be expressed as

$$q = -K_s \frac{dH}{dz} \quad (3)$$

121
 122 where $H=h+z$ (L) is the total head, and z is a vertical coordinate (L) positive upward.

123 The unsaturated soil hydraulic properties can be described according to (van Genuchten, 1980)

$$S_e(h) = \frac{\theta(h) - \theta_r}{\theta_s - \theta_r} = \frac{1}{\left(1 + |\alpha h|^n\right)^m} \quad (4)$$

$$K(\theta) = K_s S_e^{0.5} \left[1 - \left(1 - S_e^{1/m}\right)^m\right]^2 \quad (5)$$

124
 125
 126 where S_e is the effective water content, K_s is the saturated hydraulic conductivity, θ_s and θ_r denote the
 127 saturated and residual volumetric water content, respectively, and α (L^{-1}), n , and $m=(1-1/n)$ are
 128 empirical parameters. Under this formulation, van Genuchten (1980) found that the soil diffusivity,
 129 D , could be expressed as.

$$D(S_e) = \frac{(1-m)K_s}{\alpha m(\theta_s - \theta_r)} S_e^{1/2-1/m} \left[\left(1 - S_e^{1/m}\right)^{-m} + \left(1 - S_e^{1/m}\right)^m - 2 \right] \quad (6)$$

130
 131 Parlange (1975) demonstrated that, for homogeneous, uniform initial water content and infinite
 132 length soil column, S could be defined as

$$S^2(\theta_s, \theta_0) = \int_{\theta_i}^{\theta_s} D(\theta) [\theta_s + \theta - 2\theta_i] d\theta \quad (7)$$

133
 134 where θ_i is the initial volumetric water content.

135 Combining Eq. (6) and (7), we obtain

136
$$S^2 = \frac{(1-m)K_s}{\alpha m(\theta_s - \theta_r)} \int_{\theta_i}^{\theta_s} [\theta_s + \theta - 2\theta_i] S_e^{1/2-1/m} \left[\left(1 - S_e^{1/m}\right)^{-m} + \left(1 - S_e^{1/m}\right) - 2 \right] d\theta \quad (8)$$

137

138 **2.2. Estimation of the water retention curve parameters**

139 The estimation of the van Genuchten (1980) soil water retention parameters (α and n) from a single
140 upward infiltration curve measured on a finite soil column required the following steps (Moret-
141 Fernández and Latorre, 2016).

- 142 - Homogeneous, uniform initial water content close to θ_r and finite soil core was considered.
- 143 - An upward infiltration curve made by saturation conditions at the bottom of the soil sample,
144 followed by an overpressure step at the end of the water absorption process, was measured.
145 Because Eq. (1) requires infinite soil columns, only infiltration times between $t = 0$ and the
146 time just before the wetting front arrives at the top of the soil column were considered.
- 147 - The K_s was calculated by applying Eq. (3) to the overpressure step measured at the end of the
148 soil wetting process.
- 149 - By introducing the calculated K_s in Eq. (1), S and β were numerically estimated by minimizing
150 the objective function, Q , that represents the difference between Eq.(1) and the experimental
151 upward infiltration (I) data (Moret-Fernández and Latorre, 2016):

152
$$Q = \sum_{i=1}^N ((I_i - I(S, \beta, t_i)) \Delta t_i)^2 \quad (9)$$

153 where N is the number of measured (I t) values. To this end, a global optimization search
154 (Pardalos and Romeijn, 2002) was employed. The objective function was summarized as
155 contours (response surfaces) for the S - β and t - β combinations. The parameter combinations for
156 the response surface were calculated on a rectangular grid, with S , β values ranging from 0.1

157 to 2.5 and 0.3 to 1.7, respectively and t between $t = 0$ and the time just before the wetting front
158 arrive to the top of the soil column, respectively.

159 - By introducing the calculated K_s , S and β values in Eqs. (2) and (8), we obtained a system of
160 two equations with two unknown variables (α and n). This system of equations was
161 numerically solved with the R V. 3.3.1 software (The R Foundation for Statistica Computing).

162

163 **2.3. Field experiments**

164 *2.3.1. Sorptivimeter*

165 The upward infiltration curve was measured with a sorptivimeter (Moret-Fernández et al., 2016).
166 This consists in a saturated perforated base of 5 cm-diameter, that accommodates a 5 cm i.d by 5 cm-
167 high stainless steel cylinder containing the undisturbed soil sample (Fig. 1). The bottom of the
168 perforated base is connected to a Mariotte water-supply reservoir (30 cm high and 2.0 cm i.d.). A \pm
169 3.44 kPa differential pressure transducer (PT) (Microswitch, Honeywell), connected to a datalogger
170 (CR1000, Campbell Scientist Inc.), was installed at the bottom of the water-supply reservoir (Casey
171 and Derby, 2002).

172 The sorptivimeter implementation required that the perforated plus the nylon mesh base were
173 previously saturated. The measurement started when the cylinder containing the undisturbed soil
174 sample was placed on the saturated base, and finished when the wetting front arrived at the soil
175 surface. At this time, an overpressure step, ranging between 2 and 12 cm of pressure head from the
176 soil surface, was introduced by raising the water reservoir to a desired height. The saturated hydraulic
177 conductivity was calculated from the overpressure section of the cumulative absorption curve
178 according to Eq.(3). The initial and final water content were gravimetrically measured. Additionally,
179 the final water content was also calculated as the sum of the initial water content plus the water
180 absorbed by the soil at the time that a water sheet is observed on the soil surface. More details of the
181 sorptivimeter design and its implementation are summarized in Moret-Fernández et al. (2016)

182

183 *2.3.2. Field sampling and method testing*

184 The undisturbed cores were collected from consolidated soils located in two different places. The
185 first field (EEAD) is located at the dryland research farm of the Estación Experimental de Aula Dei
186 (CSIC) in the province of Zaragoza (41°44'N, 0°46'W, altitude 270 m). The climate is semiarid with
187 an average annual precipitation of 390 mm and an average annual air temperature of 14.5°C. Soil at
188 the research site is a loam (fine-loamy, mixed, thermic Xerollic Calciorthid) according to the USDA
189 soil classification (Soil Survey Staff, 1975). Selected physical and chemical properties of the soil are
190 given in Blanco-Moure et al. (2012). The study was conducted in a block with three plots (30 x 10 m²
191 per plot), which were set up on a low angle slope area (slope 0–2%) of land in 1991 within a long-
192 term conservation tillage experiment. The field was in winter barley (*Hordeum vulgare* L.)–fallow
193 rotation, and the sampling were performed conducted when the field was in the 16- to 18-mo-long
194 fallow phase of this rotation, which extends from harvest (June–July) to sowing (November–
195 December) the following year. Three different tillage management treatments, one per plot, were
196 compared: CT, RT, and NT. The CT treatment consisted of mouldboard ploughing of fallow plots to
197 a depth of 30 to 40 cm in late winter or early spring, followed by secondary tillage with a sweep
198 cultivator to a depth of 10 to 15 cm in late spring. In the RT treatment, the primary tillage was chisel
199 ploughing to a depth of 25 to 30 cm (non-inverting action), followed as in CT by a pass of the sweep
200 cultivator in late spring. The NT treatment used exclusively herbicides (glyphosate [N-(phosphorous
201 methyl)glycine]) for weed control throughout the fallow season.

202 The second field was located in the Belchite municipality (Zaragoza), also in the Middle Ebro
203 Valley (NE, Spain; 41°30'N, 0°15'W), and at 250 m above the sea level. The climate is semi-arid
204 Mediterranean, the mean rainfall is 353 mm/year (average of 50 years at 250 m above sea level), and
205 the mean annual temperature is 14.9 °C (M.A.P.A., 1987) (Table 1). Soil at the research site is a loam
206 (Calcic Petrogypsid) according to the USDA soil classification (Soil Survey Staff, 2010). The

207 lithology is a gypsum substratum alternating with carbonate units (marls and limestone) and clays
208 (Quirantes, 1978). The landscape is characterized by low hills and flat-bottomed valleys with
209 altitudes ranging from 127 to around 800 m a.s.l. Hills are occupied mainly by dwarf-scrubs of
210 *Rosmarinus officinalis* L., while uncultivated valley bottoms are occupied by *Lygeum spartum* L.
211 steppe and scarce scrub of *Salsola vermiculata* L. and *Artemisia herba-alba* Asso (Braun-Blanquet
212 and Bolòs, 1957). Land use in the area is based on a traditional agropastoral system involving dry
213 cereal croplands and extensive sheep production. Two different soil management types were
214 considered: ungrazed natural shrubland, N; and grazed shrubland, GR. The grazing treatment
215 consisted of a moderate grazing intensity (<1 head ha^{-1} year $^{-1}$) according to the traditional use in the
216 area (Pueyo, 2005). The treatments were located in two nearly flat experimental fields, separated 1
217 km one from other. Characteristics of the soils employed in the experiments are summarized in Table
218 1.

219 In all cases, the sampling points, which were located on bare soil, were uniformly distributed in the
220 plots. Six undisturbed soil cores were sampled per plot using the core method, with core dimensions
221 of 50 mm internal diameter and 50 mm-high. In the laboratory, soil cores were air dried over several
222 weeks. Once the soil samples were air dried, three replications per soil type and treatment were
223 employed to estimate the α and n with the UP method. The remaining three replications were
224 subsequently employed to estimate the van Genuchten (1980) parameters using TDR-pressure cells
225 (PC) (Moret-Fernández et. al, 2012). The volumetric water content (θ) in the pressure cell was
226 measured by TDR in the air dry soil, which corresponds to a pressure head (h) of about -166 MPa
227 (Munkolm and Kay, 2002), at soil water saturation and at pressure heads of -0.5, -1.5, 3-, -10 and -50,
228 kPa. In our case, the θ_r and θ_{sat} corresponded to the air dry soil water content and the water content at
229 saturation measured TDR. The measured pairs of values θ and h were numerically fitted with the R
230 V.3.1.1 (The R Foundation dor Statistical Computing) software to the van Genuchten (1980) model
231 (Eq. 1). To this end, θ_{sat} and θ_r were considered as known values and the α and n were estimated by

232 minimizing an objective function, $T(\alpha, n)$ that represents the difference between the simulated and
 233 the experimental data

$$234 \quad T = \sum_{i=1}^N ((\theta(h)_i - \theta(h)(\alpha, n)))^2 \quad (10)$$

235 where N is the number of measured (θ, h) values. A brute-force search was used on the optimization.
 236 Given the two unknown variables, α and n , the values of the objective functions were summarized as
 237 contours (response surfaces) for the α - n combination. The resultant response surface was calculated
 238 on a rectangular grid, with α and n values ranging from 0.01 to 10 and 1.2 to 2.2, respectively. The
 239 water retention parameters calculated with the UP method were compared to the corresponding
 240 values estimated with the TDR-pressure cell. Because UP and TDR-cell methods calculate the
 241 opposite branches of the water retention curve, the α parameters obtained from the upward
 242 infiltration measurements were converted to the corresponding drying branch using the I hysteresis
 243 index developed by Gebrenegus and Ghezzehei (2011)

$$244 \quad I = \left(\frac{r^n - 1}{\frac{n(n-1)}{r^{2n-1}} - 1} \right)^{\frac{1}{n}-1} - \left(\frac{r^n - 1}{r^n - r^{\frac{n^2}{2n-1}}} \right)^{\frac{1}{n}-1} \quad (11)$$

245 where $r = \alpha_d / \alpha_w$; and the subscripts d and w , denote drying- and wetting-curve, respectively. In the
 246 absence of measured wetting and drying water retention data, the I index was calculated as
 247 Gebrenegus and Ghezzehei (2011)

$$248 \quad I = 0.378 \ln(n) \quad (12)$$

249 As reported by Likos et al. (2014), no significant influence of the wetting-drying process on the n
 250 parameter was considered.

251 The same soil cores used to calculate the soil hydraulic properties were finally dried at 50 °C for 72
 252 h and employed to calculate the soil bulk density. Since gypsum content was relevant in the studied
 253 soils, the 50 °C temperature was used to avoid the constitutional water release by the gypsum crystal

254 because of the transformation of gypsum into bassanite or anhydrite at temperatures >50 °C (Herrero
255 et al., 2009).

256 To compare the effects of the soil type and treatment on the soil hydro-physical properties, analysis
257 of one-way variance (ANOVA) for a completely randomized design was conducted using SPSS (V.
258 13.0) statistical software. The K_s , α and n variable measured from the upward infiltration needed to
259 be normalized with the \log_{10} transformation. All treatment means were compared using Duncan's
260 multiple range test.

261

262 **3.- RESULTS AND DISCUSSION**

263 The head losses due to the water flow from the water reservoir to the sorptivimeter calculated
264 according to the sorptivimeter pipes dimensions were negligible (< 0.1 mm). As example, Figure 2
265 shows, for one of the three replications measured in each soil and treatment, the best fitting between
266 experimental and simulated upward infiltration curves and the error maps for the S - β and β - t
267 combinations. In all cases, the results showed an excellent fitting between experimental and
268 simulated upward infiltration curves ($R^2 > 0.98$), and S - β response surfaces with a unique and well
269 defined minimum. This indicated the upward infiltration times used in the experiments gave accurate
270 estimations of S and β . Similar conclusions were achieved when analysing the t - β response surfaces,
271 where the β value tended to asymptotically coalesce to a unique and well defined value. These results
272 suggested that the 5 cm-high cylinder used in the experiment was long enough for accurate estimates
273 of β . Because the S parameter is accurately derived from the early-time of the upward infiltration
274 (Moret-Fernández and Latorre, 2016), the response surfaces for the t - S combination were not
275 considered in the analysis. The β value was, in all cases, lower than 1.7, which denoted that the
276 model could satisfactorily be used to estimate the soil hydraulic properties (Lassavatore et al., 2009).
277 Except for the θ_r , β and n parameters, significant differences between the five different soils were

278 observed for K_s , S , α and θ_s (Table 2). Overall, the K_s and S values measured from the upward
279 infiltration were within the same order of magnitude as those measured in situ and in the same fields
280 and treatments with the disc infiltrometer (Moret-Fernández et al., 2011, 2013).

281 The unique minimum observed in the $T(\alpha, n)$ response surface calculated from the water retention
282 curves measured with the TDR-pressure cell indicated that total number of pairs of h - θ values used
283 in the experiments was enough to provide accurate estimates of α and n (Fig. 3). Overall, a good
284 fitting between experimental and simulated water retention curves was obtained. Significant
285 differences for the comparison between the θ_s , α and n values calculated from the TDR-pressure cell
286 measurements were observed among all treatments (Table 3).

287 A significant relationship, with a slope close to one, was observed between the n values estimated
288 with the TDR-pressure cell and the corresponding values estimated from the upward infiltration
289 curves (Fig. 4a). On average, the n values calculated from the optimized S and β data were 4.8%
290 larger than those obtained with the TDR-pressure cell. This means that the $\theta(h)$ measured with the
291 TDR-cell presented a smoother slope, which involved larger water content at more negative pressure
292 heads. As reported by Solone et al. (2012), this difference could be due to limitations of the pressure
293 plate apparatus, when the θ was measured at high pressure heads. For instance, if the time needed to
294 stabilize the water flow inside the pressure cell was not long enough, the θ measured by the pressure
295 cell at the end of the pressure step would be larger than the actual value. On the other hand, the lack
296 of data between the lowest applied pressure head (-50 kPa) and the pressure head for θ_r , could give
297 more weight to the dry end of the water retention function, making softer slopes and consequently
298 lower n values. While significant differences in n values among the different soil treatments were
299 observed in the PC (Table 2), these differences vanished in UP (Table 3). This different behaviour
300 between both methods could be explained by the higher standard deviation observed in UP, which
301 indicated that PC was less sensitive to the soil variability. This could be explained by the soil

302 flooding conditions imposed in the pressure cells that may collapse the more unstable soil aggregates,
303 (Moret-Fernández et al., 2016a), homogenize the soil porosity, and consequently, decrease the
304 standard deviation of the calculated n values. All these problems probably vanished with the upward
305 infiltration method, where the bulk soil was not waterlogged and the wetting process included all soil
306 pressure heads from the residual to the saturated water content.

307 Overall, the α values for the drying branch of $\theta(h)$ calculated from the upward infiltration
308 measurements were larger than those calculated with the TDR-pressure cell (Fig. 4b). This means
309 that the soil with UP showed higher pore volume at the wet end of the soil water retention curve
310 (Ahuja et al., 1998) (Fig. 5). The difference between the maximum and minimum average α values
311 measured for the five soils with the PC and the UP method were 0.021 and 0.14 cm⁻¹, respectively.
312 These results indicate that the UP method was more sensitive to detect differences in the α parameter.
313 This differential behaviour between both methods could be again explained by the wetting process up
314 to saturation used in the TDR-pressure cell, which may have an important influence on the structural
315 component of the soil, and consequently on the α parameter. As reported by Moret-Fernández et al.
316 (2016a), the soil waterlogged conditions in the pressure cell can collapse the more unstable
317 macropores and increase the volume of the smaller ones, causing a decrease and a homogenization of
318 the α value. Although these authors observed that this effect was more significant in freshly tilled
319 soils, this phenomenon was also evident in consolidated soils. These soil dynamics may be
320 minimized by the upward infiltration technique, where the S and β are estimated from the upward
321 infiltration curve, before the soil is saturated. This process may prevent collapsing the more unstable
322 soil pores, which resulted in increasing α values. This lack of correlation may be also due to the
323 different process considered for measuring α (wetting vs. draining), where an indirect confirmation
324 for this is given by the good correlation found for n that, as commonly known, is less affected by
325 hysteresis. The larger hysteresis index obtained in the experimental soils might also be related with

326 the cracks that can appear after air drying the soil or the preferential channels of the undisturbed soil
327 samples, which are not taken into account in the hysteresis models.

328

329 **4.-CONCLUSIONS**

330 This work shows that the method recently developed by Moret-Fernández and Latorre (2016),
331 which determines the α and n parameters from the S and the β values calculated from the inverse
332 analysis of an upward infiltration curve, can be satisfactorily applied to undisturbed soil cores of 5
333 cm height. The differences in the α and n values observed between both methods could be attributed
334 to limitations of the PC method, in which the soil flooding process used in the pressure cells, together
335 with the limited soil pressure heads employed in this method, could result in an underestimation of
336 the α and n value. In conclusion, this work used an inexpensive, fast and simple to implement method
337 that, unlike to the current techniques, allows estimating the hydraulic properties of undisturbed soil
338 samples using the 5 cm-high cylinders commonly used to measure the soil bulk density. A free
339 application to apply this method will be available in the Soil and Water Infiltration web site
340 (<http://swi.csic.es>).

341

342 **Acknowledgments**

343 This research was supported by the Ministerio de Economía y Competitividad of Spain (CGL2014-
344 53017-C2-1-R and CGL2016-80783-R) and Aragon Regional Government and La Caixa (GA-
345 LC020/2010; 2012/ GA LC 074). The authors are grateful to the Área de Informática Científica de la
346 SGAI (CSIC) for their technical support in the numerical analysis and to R. Gracia and M.J. Salvador
347 for technical help in several aspects of this study.

348

349 **References**

350 Ahuja LR, Fiedler F, Dunn GH, Benjamin JG, Garrison A (1998) Changes in soil water retention
351 curves due to tillage and natural reconsolidation. *Soil Science Society of America Journal* **62**,
352 1228-1233.

353 Arya LM (2002). Wind and hot-air methods, in: Dane, J.H., and G.C. Topp, (ed.). *Methods of Soil*
354 *Analysis. Part.4. SSSA Book Series No. 5. Soil Sci. Soc. Am., Madison, WI.*

355 Blanco-Moure N, Angurel LA, Moret-Fernández D, López MV (2012). Tensile strength and organic
356 carbon of soil aggregates under long-term no tillage in semiarid Aragon (NE Spain).
357 *Geoderma* **189--190**: 423-430.

358 Braun-Blanquet J, Bolòs O (1957). Les groupements végétaux du Bassin Moyen de l'Ebre et leur
359 dynamisme. [Vegetation communities in the Central Ebro Valley and their dynamics.] *Anales*
360 *de la Estación Experimental de Aula Dei* **5**: 1–266.

361 Casey FXM, Derby NE (2002). Improved design for an automated tension infiltrometer. *Soil Science*
362 *Society of America Journal*, **66**: 64–67.

363 Gardner WR, FJ Miklich (1962). Unsaturated conductivity and diffusivity measurements by a
364 constant flux method. *Soil Science* **93**: 271–274.

365 Gebrenegus T, Ghezzehei TA (2011). An index for degree of hysteresis in water retention. *Society of*
366 *American Journal* **75**; 2122–2127

367 Han XW, Shao M, Horton R (2010). Estimating van Genuchten model parameters of undisturbed
368 soils using an integral method. *Pedosphere* **20**: 55-62.

369 Haverkamp R, Ross PJ, Smettem KRJ, Parlange JY (1994). Three dimensional analysis of infiltration
370 from the disc infiltrometer. Part 2. Physically based infiltration equation. *Water Resources*
371 *Research* **30**: 2931-2935.

372 Herrero J, Artieda O, Hudnall WH. 2009. Gypsum, a tricky material. *Soil Science Society of America*
373 *Journal* **73**: 1757–1763.

374 Hudson DB, Wierenga PJ, Hills RG (1996). Unsaturated hydraulic properties from upward flow into
375 soil cores. *Society of American Journal* **60**: 388-396.

376 Klute AJ (1952). Some theoretical aspects of the flow of water in unsaturated soils. *Soil Science*
377 *Societe of America Proceedings* **16**:144-148.

378 Lassabatere L, Angulo-Jaramillo R, Soria-Ugalde JM, Simunek J, Haverkamp R (2009). Numerical
379 evaluation of a set of analytical infiltration equations. *Water Resources Research*, **45**,
380 doi:10.1029/2009WR007941.

381 Lichtner PC, Steefel CI Oelkers EH (1996). Reactive Transport in Porous Media. Mineralogical
382 Society of America , p. 5.

383 Likos WJ, Lu N, Gogt JW (2014). Hysteresis and uncertainty in soil water-retention curve
384 parameters. *Journal of Geotechnical and Geoenvironmental Engineering*. Doi:
385 10.1061/(ASCE)GT.1943-5606.0001071.

386 Moret-Fernández D, Blanco N, Martínez-Chueca V, Bielsa A (2013). Malleable disc base for direct
387 infiltration measurements using the tension infiltrometry technique. *Hydrological Processes*.
388 **27**: 275–283.

389 Moret-Fernández D, Pueyo Y, Bueno CG, Alados CL, 2011. Hydro-physical responses of gypseous
390 and non-gypseous soils to livestock grazing in a semiarid region of NE Spain. *Agricultural*
391 *Water Management* **98**: 1822–1827.

392 Moret-Fernández D, Latorre B, 2016. Estimate of the soil water retention curve from the sorptivity
393 and β parameter calculated from an upward infiltration experiment *Journal of Hydrology*
394 <http://dx.doi.org/10.1016/j.jhydrol.2016.11.035>.

395 Moret-Fernández D, Peña-Sancho C, López MV (2016a). Influence of the wetting process on
396 estimation of the water-retention curve of tilled soils. *Soil Research* DOI: 10.1071/SR15274

397 Moret-Fernández D, Latorre B, Peña-Sancho C, Ghezzehei TA (2016b). A modified multiple tension
398 upward infiltration method to estimate the soil hydraulic properties. *Hydrological Processes*
399 DOI: 10.1002/hyp.10827.

400 Moret-Fernández D, Vicente J, Latorre B, Herrero J, Castañeda C, López MV. (2012). A TDR
401 pressure cell for monitoring water content retention curves on undisturbed soil samples.
402 *Hydrological Processes* **26**: 246–254.

403 Munkholm LJ, Kay BD (2002). Effect of water regime on aggregate-tensile strength, rupture energy,
404 and friability. *Soil Science Society of America Journal* **66**: 702–709.

405 Pardalos PM, Romeijn HE (Eds.) (2002). Handbook of global optimization (Vol. 2). Springer. Berlin.

406 Parlange JY (1975). On solving the flow equation in unsaturated flow by optimization: Horizontal
407 infiltration. *Soil Science Society of American Journal* **39**: 415-418.

408 Peña-Sancho, C., Ghezzehei, T.A., Latorrea, B., Moret-Fernández, D. 2017. Water absorption-
409 evaporation method to estimate the soil hydraulic properties. *Hydrological Sciences Journal*
410 (accepted).

411 Pueyo Y, Moret-Fernández D, Saiz H, Bueno CG, Alados CL (2013). Relationships between plant
412 spatial patterns, water infiltration capacity, and plant community composition in semi-arid
413 mediterranean ecosystems along stress gradients. *Ecosystems* **16**: 452–466.

414 Quirantes J (1978). Estudio sedimentológico y estratigráfico del Terciario continental de los
415 Monegros. [Sedimentological and stratigraphic study of the Tertiary continental of the
416 Monegros.] Institución Fernando el Católico, Zaragoza.

417 Simunek J, Wendroth O, van Genuchten MT (1998). Parameter estimation analysis of the
418 evaporation method for determining soil hydraulic properties. *Soil Science Society of America*
419 *Journal* **62**: 894-895.

420 Solone R, Bittelli M, Tomei F, Morari F (2012). Errors in water retention curves determined with
421 pressure plates: Effects on the soil water balance. *Journal of Hydrology* **470**: 65-75.

- 422 Shao M, Horton R (1998). Integral method for estimating soil hydraulic properties. *Soil Science*
423 *Society of America Journal* **62**: 585-592.
- 424 Van Genuchten MT (1980). A closed form equation for predicting the hydraulic conductivity of
425 unsaturated soils. *Soil Science Society of America Journal* **44**: 892– 898.
- 426 Young MH, Karagunduz A, Siumunek J, Pennell, KD (2002). A modified upward infiltration method
427 for characterizing soil hydraulic properties. *Soil Science Society of America Journal* **66**: 57–
428 64.

Figure captions

429

430

431 **Figure 1.** Sorptivimeter scheme

432

433 **Figure 2.** Experimental (cycles) and best optimization (line) of the upward infiltration curves, and the
434 error maps for the S - β and β - t combinations estimated from minimization of the Q function for one
435 of the four replications measured in each soil and treatment. CT, conventional tillage; RT, reduce
436 tillage, NT, no tillage; natural shrubland, N; and grazed shrubland, GR. Red line in β - t
437 combinations denotes the 0.02 contour line.

438

439 **Figure 3.** Experimental (cycles) and best optimization (line) of the water retention curves and error
440 maps for the α - n combination estimated from minimization of the T function for one of the four
441 replications measured in each soil and treatment. CT, conventional tillage; RT, reduce tillage, NT,
442 no tillage; natural shrubland, N; and grazed shrubland, GR.

443

444 **Figure 4.** Relationship between the n (a) and α (b) values estimated with upward infiltration for the
445 drying branch of the water retention curve and the corresponding values measured with TDR-
446 pressure cell method.

447

448 **Figure 5.** Averaged water retention curve estimated with the pressure cell (PC) and upward
449 infiltration (UP) methods on conventional tillage (CT), reduce tillage (RT), no tillage (NT), natural
450 shrubland (N) and grazed shrubland (GR) treatments.

451

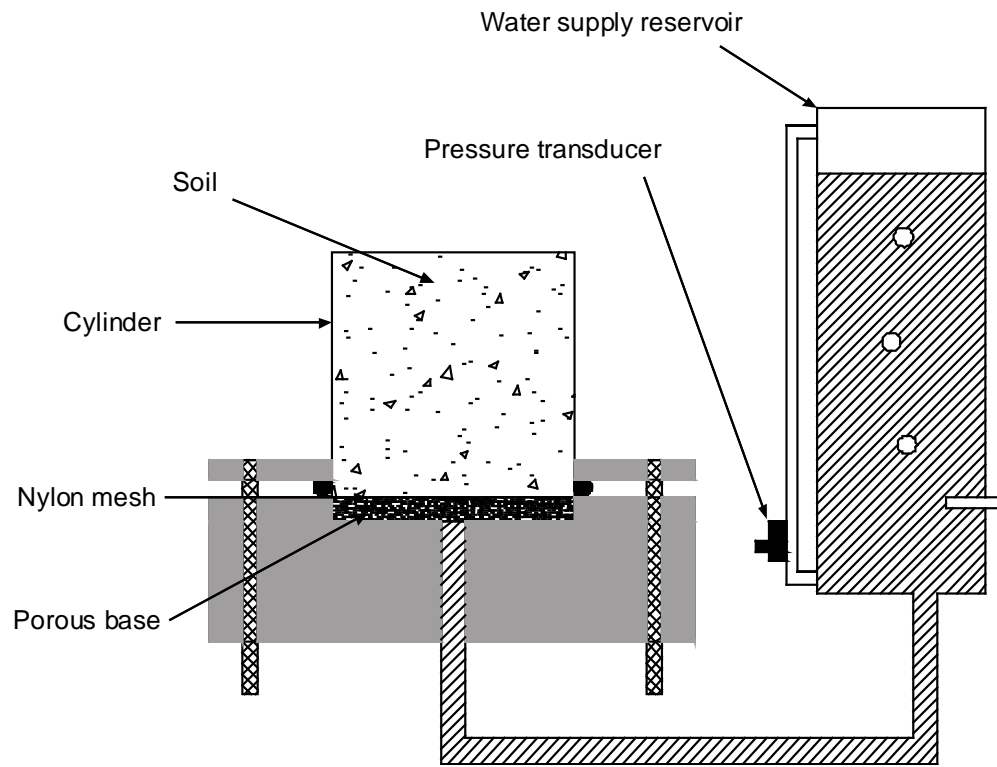


Figure 1. Sorptivimeter scheme

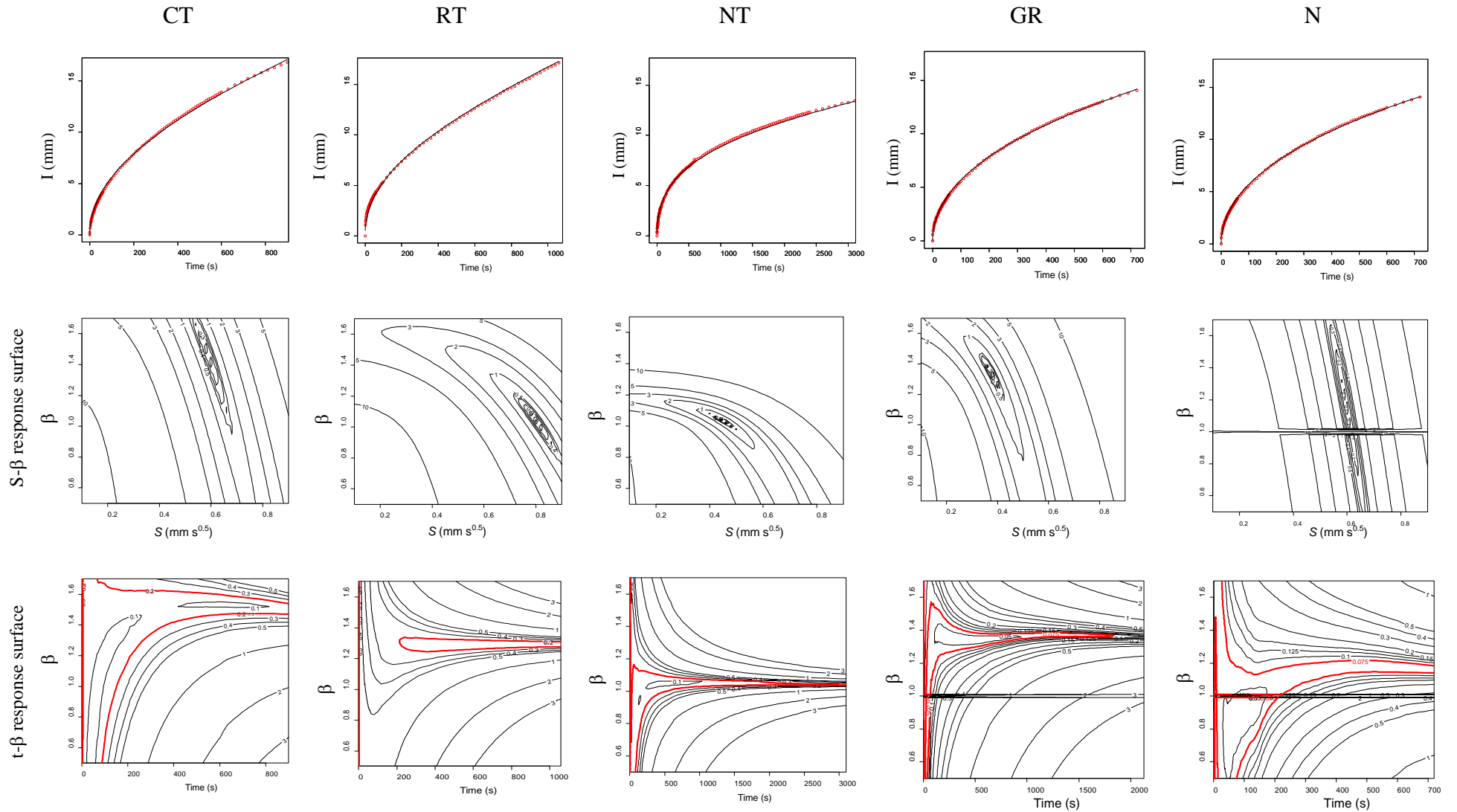


Figure 2. Experimental (cycles) and best optimization (line) of the upward infiltration curves, and the error maps for the S - β and β - t combinations estimated from minimization of the Q function for one of the four replications measured in each soil and treatment. CT, conventional tillage; RT, reduce tillage, NT, no tillage; natural shrubland, N; and grazed shrubland, GR. Red line in β - t combinations denotes the 0.02 contour line.

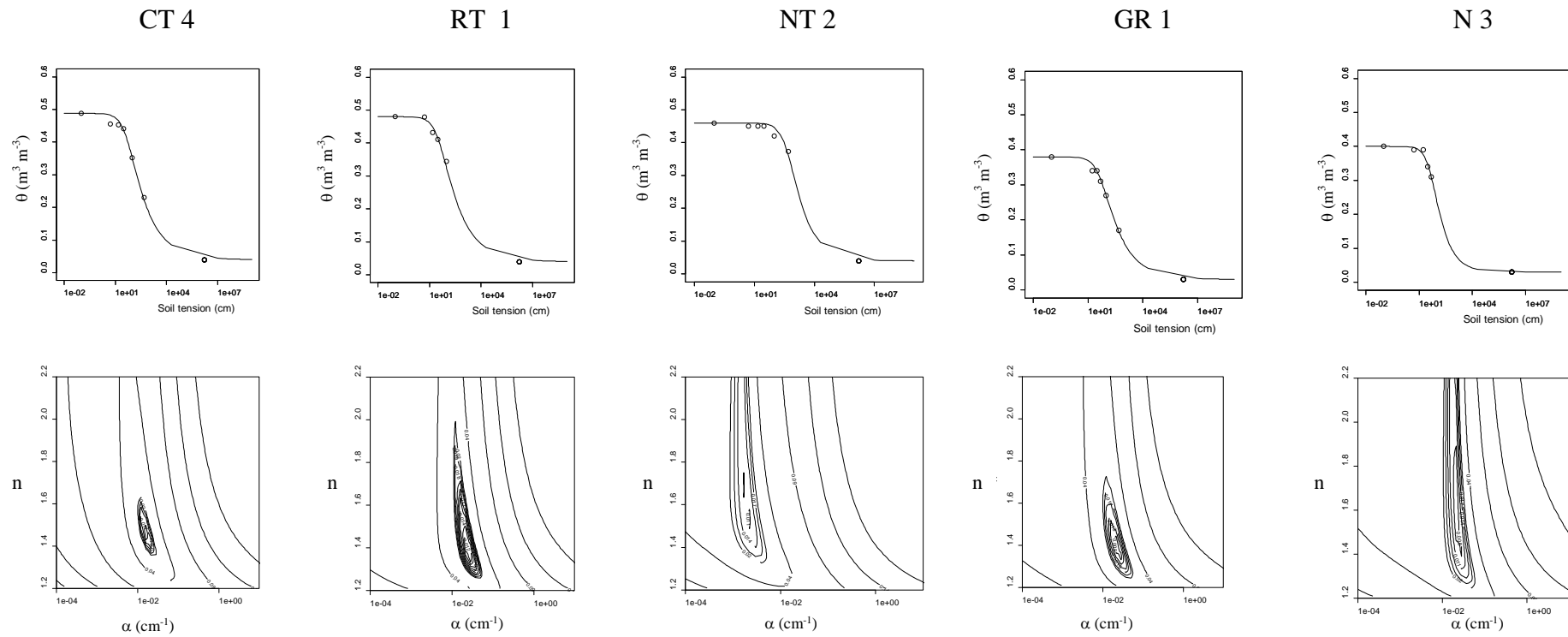


Figure 3. Experimental (cycles) and best optimization (line) of the water retention curves and error maps for the α - n combination estimated from minimization of the T function for one of the four replications measured in each soil and treatment. CT, conventional tillage; RT, reduce tillage, NT, no tillage; natural shrubland, N; and grazed shrubland, GR.

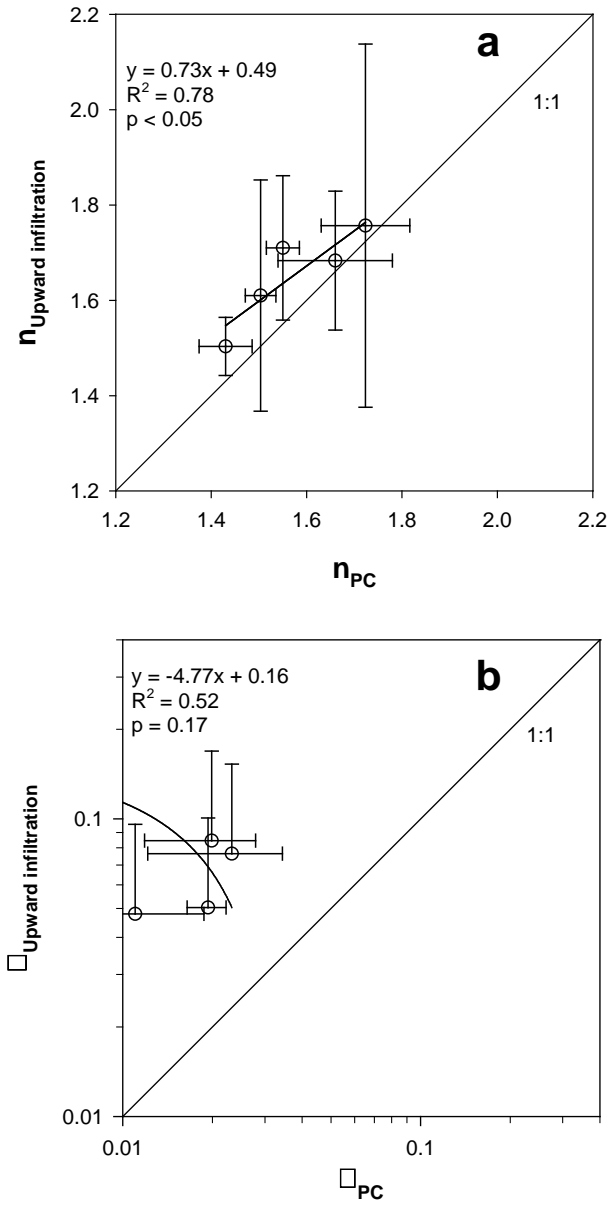


Figure 4. Relationship between the n (a) and α (b) values estimated with upward infiltration for the drying branch of the water retention curve and the corresponding values measured with TDR-pressure cell method.

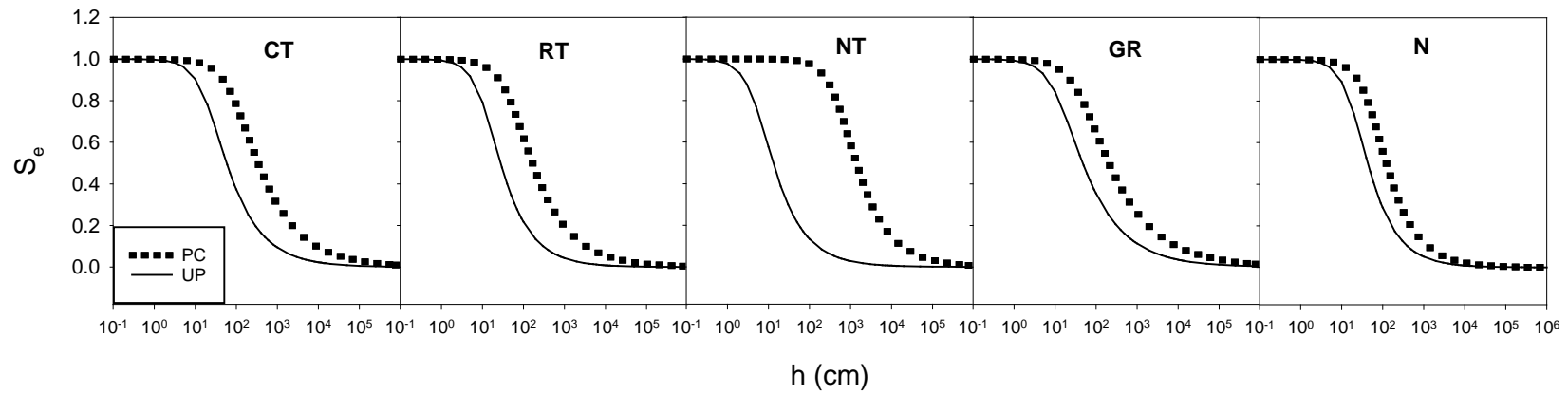


Figure 5. Averaged water retention curves estimated with the pressure cell (PC) and upward infiltration (UP) methods on conventional tillage (CT), reduce tillage (RT), no tillage (NT), natural shrubland (N) and grazed shrubland (GR) treatments.

1 **Table 1.** Gypsum, CaCO₃, organic carbon (OC) contents, averaged soil bulk density (ρ_b) and textural characteristics of
 2 the studied soils (0-5 cm depth).

Location	Management	Gypsum	CaCO ₃	OC	ρ_b	Sand	Silt	Clay	Textural classification ¹
		%			g cm ⁻³	%			
EEAD	CT	4.87	46.2	1.07	1.31	28.7	46.3	25.0	Loam
	RT	4.14	46.6	1.11	1.32	31.8	43.9	24.3	Loam
	NT	4.43	47.3	1.33	1.37	31.3	45.1	23.6	Loam
Codo	Grazed	43.78	7.07	0.46	1.46	42.8	43.4	13.8	Loam
	Ungrazed	40.28	9.23	0.43	1.44	42.2	40.9	16.9	Loam

3 ¹ USDA classification

4
5

Table 2. Average and standard deviation (within parenthesis) values of the saturated hydraulic conductivity (K_s), sorptivity (S), β parameter, and saturated (θ_s) and residual (θ_r) volumetric water content measured from the upward infiltration experiments, and the α value for a wetting (α_w) and drying (α_d) process and n parameters of the van Genuchten (1980) model calculated from K_s , S and β measured for the different treatments: CT, conventional tillage; RT, reduce tillage, NT, no tillage; ngrazed natural shrubland, N; and grazed shrubland, GR. Within the same column, different letters indicate significant differences among soil treatments ($p < 0.05$).

Treatments	K_s	S	β	θ_s	θ_r	α_w	α_d	n
	mm s ⁻¹	mm s ^{-0.5}		m ³ m ⁻³			cm ⁻¹	
CT	0.019 (0.005) a	0.69 (0.10) a	1.25 (0.24) a	0.51 (0.03) a	0.04 (0.001) a	0.09 (0.02) b	0.05 (0.01) b	1.61 (0.24) a
RT	0.029 (0.008) a	0.68 (0.11) a	1.14 (0.14) a	0.50 (0.01) a	0.04 (0.001) a	0.17 (0.02) b	0.08 (0.01) b	1.71 (0.15) a
NT	0.023 (0.008) a	0.37 (0.04) bc	1.17 (0.14) a	0.45 (0.02) b	0.03 (0.001) a	0.37 (0.17) a	0.19 (0.08) a	1.68 (0.15) a
GR	0.006 (0.004) b	0.27 (0.09) c	1.34 (0.07) a	0.40 (0.02) c	0.04 (0.001) a	0.15 (0.02) b	0.08 (0.01) b	1.50 (0.06) a
N	0.032 (0.039) a	0.53 (0.18) ab	1.14 (0.31) a	0.41 (0.03) c	0.03 (0.001) a	0.10 (0.04) b	0.05 (0.02) b	1.76 (0.38) a

Table 3. Average and standard deviation (within parenthesis) values of the saturated (θ_s) and residual (θ_r) volumetric water content, α and n parameter of the water retention curve calculated from the TDR-pressure cell data measured for the different treatments: CT, conventional tillage; RT, reduce tillage, NT, no tillage; grazed natural shrubland, N; and grazed shrubland, GR. Within the same column, different letters indicate significant differences among soil treatments ($p < 0.05$).

Treatments	θ_s	θ_r	α	n
	$\text{m}^3 \text{m}^{-3}$	$\text{m}^3 \text{m}^{-3}$	cm^{-1}	mm s^{-1}
CT	0.47 (0.03) b	0.04 (0.001) a	0.011 (0.008) ab	1.50 (0.03) c
RT	0.50 (0.01) a	0.04 (0.001) a	0.020 (0.008) a	1.55 (0.01) bc
NT	0.47 (0.01) b	0.03 (0.001) a	0.002 (0.001) b	1.66 (0.12) ab
GR	0.36 (0.01) c	0.04 (0.001) a	0.023 (0.011) a	1.43 (0.06) c
N	0.38 (0.01) c	0.03 (0.001) a	0.019 (0.003) a	1.72 (0.09) a